Optochemical control of cell contractility at single cell resolution during tissue morphogenesis

Deging Kong [(1)], Fred Wolf [(2)], Jörg Großhans [(1)]

(1) Institute for Developmental Biochemistry, University of Göttingen, Justus-von-Liebig Weg 11, 37077 Göttingen, Germany.
(2) Max Planck Institute for Dynamics and Self-Organization (MPI-DS), Bernstein Center for Computational Neuroscience Göttingen, Faculty of Physics, University of Göttingen, Am Faßberg 17, 37077 Göttingen, Germany.

Abstracts

Spatial and temporal dynamics in cell contractility plays a central role in tissue morphogenesis, wound healing and cancer invasion. Here we report a simple and minute-scale optochemical method to induce reversible cell contraction at single cell resolution during epithelial tissue morphogenesis. We employed the photolabile Ca^{2+} chelator *o*-nitrophenyl EGTA to induce a burst of intracellular free Ca^{2+} by UV laser. Ca^{2+} bursts appear within seconds and are restricted to the targeted cell. Cell contraction followed within a minute. Increased Ca^{2+} levels and contraction are reversible and the target cells further participated in tissue morphogenesis. Our approach can be easily adapted to many experimental systems and species, since no specific genetic elements are required and a widely used chemical is employed.

Introduction

Contractility underlies manifold processes in cell and tissue morphogenesis, including cell migration, cell shape changes, or junction collapse[1-4]. In epithelial tissues, cell contractility is transmitted to neighboring cells by mechanical pulling on neighbors via adherens junctions. The mechanical link may elicit a specific response in neighbors and may thus positively or negatively affect contractility in neighbors in a non autonomous manner[5]. Within a tissue, these cell-cell interactions may contribute to emergent tissue behavior, such as folds and furrows. The function of such mutual

cell-cell interactions is difficult to study by classical genetic approaches. What is needed are acute interventions with high temporal and spatial resolution, ideally in the scale of seconds and individual cells.

Optogenetic approaches for control the cell contractility have recently been developed. Cell contractility can be inhibited by optically induced membrane recruitment of $PI(4,5)P_2$ leading to interference with phosphoinositol metabolism and subsequent suppression of cortical actin polymerization[6]. Optical activation of contractility has been achieved by light-induced activation of the Rho-Rok pathway, which controls to Myosin II based contractility[7,8]. Despite their effectiveness, optogenetic methods require expression of modified proteins including light-sensitive and dimerization domains, which need to be introduced into the genetic background of the experiment. Furthermore, the chromophores absorb light in the visible spectrum, which leads to restrictions in the choice of labelling for tracking of cells or cellular structures.

Optochemical methods represent an alternative to genetically encoded sensor and effector proteins. Intracellular calcium ions (Ca^{2+}) are known to be an important regulator of contractility in many cell types beside their central role in muscle contraction, such as in cultured epithelial cells[9], dorsal closure[10], neural tube closure[11,12] and folding morphogenesis of the neural plate[13]. Tissue wide increase of intracellular Ca^{2+} activates Myosin II and impairs egg chamber elongation in *Drosophila* oogenesis[14]. Furthermore a transient increase in Ca^{2+} concentration induces apical constriction in cells of the neural tube in *Xenopus*[15]. The molecular mechanism has remained unclear for how Ca^{2+} leads to contraction in non-muscle cells. Optochemical methods for release of Ca^{2+} to modulate intracellular ions concentration are well established and widely employed in the fields of neurobiology[16]. Here we report an Ca^{2+} uncaging method to control epithelial cell contractility in the scale of seconds and at single cell resolution during tissue morphogenesis in *Drosophila* embryos.

Results

Uncaging induces a rapid Ca^{2+} burst in epithelial cells in *Drosophila* embryos.

Photo-induced uncaging of the Ca^{2+} chelator *o*-nitrophenyl EGTA (NP-EGTA)[17] (Fig. 1A) is widely used in neurobiology for the modulation of intracellular Ca^{2+} concentration[18,19]. Here, we employed the membrane-permeant acetoxymethyl (AM) ester derivative, which complexes Ca^{2+} once the AM moiety is removed by intracellular esterases. Following microinjection into staged embryos, uncaging was induced in the focal volume of a pulsed 355 nm laser beam (Fig. 1B). In our setting, the light paths of the UV laser and the recording laser in the visible spectrum were controlled independently, which allows concomitant uncaging and imaging, for example. We conducted our experiments in the lateral epidermis of Drosophila embryos during gastrulation stage. The epidermis during this stage constitutes a columnar epithelium with a cell diameter in the range of about 8 µm and cell height of about 25 µm.

We employed a genetically encoded Ca^{2+} sensor protein, GCaMP6, to visualize and assess changes of intracellular Ca^{2+} dynamics following uncaging. Embryos expressing a membrane bound, myristoylated variant of GCaMP6[20] were injected with NP-EGTA-AM and subjected to uncaging. We observed a transient increase of GCaMP6 fluorescence within a second specifically in the cell targeted with UV light pulses (Fig. 1C). Quantification showed a fourfold increase of GCaMP fluorescence (F/F0) after two seconds. Afterwards, the GCaMP fluorescence gradually decreased to initial levels within a few minutes (Fig. 1E). We did not detect an increase of GCaMP fluorescence after UV exposure in control embryos injected with buffer only (Fig. 1D, E).

The increase in Ca^{2+} sensor signal was restricted to the single target cell. (Fig. 1C). Ca^{2+} sensor signal in the next neighbors and next-next neighbors showed fluctuations, which did not change over time and were comparable to control embryos (Fig. 1F). In summary, our experiments show that epithelial tissue in *Drosophila* embryos are susceptible to Ca^{2+} uncaging. Uncaging leads to a reversible, second-scale increase of intracellular Ca^{2+} levels restricted to the target cell. The magnitude of

the Ca^{2+} increase is comparable to what was previously reported for neuronal cells[19].

Ca^{2+} bursts induce a transient cell contraction.

We next investigated the consequence of Ca^{2+} bursts on cell shape. We conducted uncaging in embryos expressing E-Cad-GFP, which labels adherens junctions and thus cell junctions at a subapical position. Strikingly, we detected a contraction of the target cell to about half of the cross-sectional area (Fig. 2A). Target cells in control embryos injected with buffer remained largely unaffected (Fig. 2B). This was confirmed by quantification of the cross sectional areas. Similar to unexposed cells, target cells in buffer-injected embryos undergo regular cell shape changes with an amplitude of about 10–20% (Fig. 2C and S1B)[21,22]. All target cells with Ca^{2+} bursts contracted by about 50% within 1–2 minutes (Fig. 2C and S1A). After 3 minutes, some of the target cells started to relax, albeit not to their original cross-sectional area in 5 minutes (Fig. S1A).

Exposure to UV laser and Ca^{2+} uncaging did not affect further development of the target cells and surrounding tissue. We tracked target cells over an extended period of 15 min by time lapse imaging (Fig. 2D, E). Following initial contraction during the first two minutes after UV laser exposure, the target cell relaxed to almost initial size and showed typical oscillations with periods of a few minutes and amplitudes of 10–20% (Fig. 2D, E)[21,22]. We did not observe that target cells were extruded or got lost from epithelia tissue. This behavior indicates that the Ca^{2+} induced contraction was transient and target cells remained integrated in the epithelial tissue (Fig. 2D).

Modulation of UV laser exposure

We aimed at modulating contractility by varying the focal volume of the UV laser (spot radius). Variation of laser power or illumination time proved to be difficult, since either the response got lost or turn out to be too strong. We observed a faster response in contraction with an increase in focal volume. Spot radius of 4 or 1 initiated contraction within about 1 or 2.5 min, respectively. With both settings, a final contraction of about half was reached after 2.5 min or 4–5 min, respectively (Fig. 3A).

The two target cells were exposed to UV laser one by one within 10 seconds and varying focal volumes (Fig. 3B, 3C, Supp. movie 3). The larger focal volume by a larger spot radius led a faster response but not a higher degree of contraction by the cell. In any case, our experiments indicate that the dynamics of contraction can be modulated by varying the uncaging settings.

Role of Myosin II in Ca^{2+} induced cell contraction.

Multiple mechanisms are conceivable for Ca^{2+} induced cell contraction. Given the time scale in the minute range, it is unlikely that slow transcriptional or translational responses is involved. It is unlikely that Ca^{2+} directly activates contraction similar to its role in muscle cells due to the time lag between Ca^{2+} increase and contraction of the cell. In principle, a change in cell volume may involve Ca^{2+} induced efflux of water, for example. Alternatively, Ca^{2+} may activate myosin II, comparable to what has been reported for the *Drosophila* egg chamber[14]. Myosin II may be activated via Rho-Rok signaling or via Ca^{2+} dependent protein kinases or phosphatases, such as myosin light chain kinase (MLK)[23].

As the first step for investigating the mechanism of Ca^{2+} induced cell contraction, we imaged myosin II dynamics following uncaging in embryos expressing E-Cad-GFP to label cell-cell contacts and sqh-mCherry (myosin regulatory light chain) (Fig. 4). sqh-mCherry fluorescence is a direct indicator of active myosin II mini filaments, which are visible as clusters. Myosin II is found at the adherens junctions (junctional pool) and at the apical cortex (medial pool), where it is responsible for apical constriction [24]. We focused on the medial pool of myosin II. Due to bleaching of the sqh-mCherry signal in target cells, we normalized fluorescence to the time after UV exposure in embryos with and without uncaging. We observed an increase of sqh-mCherry fluorescence after about 0.5 to 1 min in embryos with the cage and a continuous drop of fluorescence in control embryos (Fig. 4C). These observations indicate that Ca^{2+} uncaging triggers myosin II activation in the same time scale as cell contraction.

Discussion

We developed and validated Ca^{2+} uncaging as an optochemical method to induce contraction in epithelial tissues with precise temporal and spatial control. This approach enables us to induce Ca^{2+} bursts in selected single cells within seconds and induce contraction to about half of the cross sectional area within 1 minute. The induced contraction is reversible and does not perturb tissue integrity. To our best knowledge, this is the first report for optically controlled cell contraction in minute scale and at single cell resolution in vivo during epithelial tissue morphogenesis.

The optochemical system that we use is based on photolabile Ca^{2+} chelators and a pulsed UV laser. The cage compound “NP-EGTA, AM” is cell-permeant. This allows convenient application on whole tissues. The 355nm UV laser is compatible with modern objectives and can be mounted on conventional live imaging microscopes. The dose of UV light depends on factors like light scattering by the tissue and thickness of the sample and needs to be carefully titrated for the experimental system. Using Ca^{2+} sensor proteins eases this task.

Importantly, Ca^{2+} uncaging does not require any genetically encoded protein, thus accelerating the generation of stocks, e. g. when comparing wild type and mutants, and opening its application to the manifold experimental systems with low genetic tractability. Furthermore, Ca^{2+} uncaging does not block any part of the visible spectrum as it relies on UV light. This allows for more options in the recording of cell and tissue behavior with all available fluorescent protein tags from CFP to RFP.

Ca^{2+} uncaging is particularly suitable for study of tissue morphogenesis. Specifically, intercellular coupling between neighboring cells poses a challenge onto interpretation of the data in tissue morphogenesis, as the cause and consequence cannot be easily distinguished. Disruption of the cyclic regulatory loops by acute interference is mandatory for dissecting functional dependencies. Although the mechanistic details for Ca^{2+} induced contraction need to be resolved, UV induced Ca^{2+} uncaging allows interference with the mechanics of tissues with appropriate temporal and high spatial resolution. The method can be applied to a wide range of

processes and organisms and should greatly improve our study for the role of cell contractility and the tissue mechanics during morphogenesis.

Materials and Methods

Fly Strains

Fly stocks were obtained from the Bloomington Drosophila Stock Center, if not otherwise noted and genetic markers and annotations are described in Flybase[25]. Following transgenes were used UASp-GCaMP6-myr[20], E-Cadherin-GFP[26], ubiquitin-E-Cadherin-GFP, Sqh-mCherry[24,27] and Mat-Gal4-67,15 (St. Johnston / Cambridge).

Ca^{2+} uncaging and imaging

NP-EGTA, AM (2 mM, Invitrogen) was prepared in 1X injection solution (180 mM NaCl, 10 mM HEPES, 5 mM KCl, 1 mM $MgCl_2$ [pH 7.2])[10]. Embryos (2–2.5 hours at 25°C) were collected for injection. Embryos were incubated at 25°C in dark about 10–20 min prior to uncaging. We employed a 355 nm pulsed YAG laser (DPSL-355/14, Rapp OptoElectonic) mounted on the epiport. We illuminated under the 'Click and Fire' Mode on the 'REO-SysCon-Zen' platform (Rapp OptoElectonic), while a movie was recorded on a spinning disc microscope (Zeiss, 100x/oil, NA1.4) with an emCCD camera (Photometrics, Evolve 512). The intensity of the UV laser was adjusted so that no morphological changes were induced in 1X injection solution injected embryos. The laser was applied for 1.5 seconds (around 300 pulses) per cell with 2.5% laser power (~0.5 mJ/cell). For the images in Fig. 2 and 3, axial stacks of 3–4 images with 0.5 µm step size were recording. For myosin II dynamics, axial stacks of 3–4 image with 1 µm step size were recording. The recording started about 0.5 min after Ca^{2+} uncaging. For variation of the focal volume for uncaging, the parameter 'spot-radius' was changed on the 'REO-SysCon-Zen' platform (Rapp OptoElectonic).

Image processing and analysis

The fluorescence intensity of GCaMP6-myr (in Fig. 1) was measured manually with ImageJ/Fiji [28]. The integrated density (a.u.) was measured along the cell membrane

and normalized by the cell membrane length (μm) to get the normalized fluorescence intensity I_t. The background I_b was from the integrated density (a.u.) which are measured from the cytoplasm and normalized by the measurement length (μm). The normalized GCaMP6 intensity fold increase was calculated as follows:

$$F/F_0 = (I_t - I_b) / (I_{-1} - I_{-1b})$$

Where I_t is the normalized intensity at time t, I_b is the normalized intensity of the background at time t. I_{-1} is the normalized intensity at 1 second before UV illumination, I_{-1b} is the normalized intensity of the background at 1 second before UV illumination.

Image stacks were projected by the “Max Intensity” option and segmented with “Tissue Analyzer” [29] in ImageJ/Fiji. Cell area measurements were carried out with ImageJ/Fiji. In movie 3, the Z-projected images were stabilized with “Image Stabilizer” [30]. The image stacks from sqh-mCherry embryos were projected with the “Max Intensity” option. Medial myosin II intensity (in Fig. 4) was measured manually with ImageJ.

Acknowledgements

We are grateful to Marion Silies, Stefan Luschnig, Adam Martin, and Daniel St Johnston for materials. We acknowledge service support from the Bloomington Drosophila Stock Center (supported by NIH P40OD018537). This work was in part supported by the Göttingen Centre for Molecular Biology (funds for equipment repair) and the Deutsche Forschungsgemeinschaft (DFG, FOR1756 GR1945/6-1/2, SFB937/TP10 and equipment grant INST1525/16-1 FUGG).

Author contributions

DK conducted the experiments and analyzed the data. FW, JG conceived and supervised the study and acquired funding. DK, JG wrote the manuscript.

Figure legend

Figure 1 Uncaging induces rapid intracellular Ca^{2+} concentration increase in epithelial target cells. (A) Structure of the cage compound. NP-EGTA complexes with Ca^{2+}. UV illumination cleaves the compound and releases free Ca^{2+}. The photo-labile bond is indicated in red. **(B)** Experimental scheme for Ca^{2+} uncaging in *Drosophila* embryos. "NP-EGTA, AM" was injected into the staged embryos. Following a brief incubation, a selected cell was targeted by a UV laser. Light paths for imaging and UV uncaging were controlled independently. Target cell is indicated in blue. **(C, D)** Images from time lapse recording of embryos (stage 7) expressing a membrane bound Ca^{2+} sensor (GCaMP6-myr) and injected with (C) 2 mM "NP-EGTA, AM" or (D) with buffer (control). Scale bar 10 µm. **(E)** Fluorescence of GCaMP sensor in the target cell normalized to initial value. Mean (bold line, 3 cells in 3 embryos) with standard error of the mean (ribbon band). **(F)** Fluorescence of GCaMP sensor in target cell, 3 next neighbors and 3 non-immediate neighbors. Target cell (red), next neighbors (green), next-next neighbors (orange). Scale bar 10 µm.

Figure 2: Ca^{2+} uncaging induces cell contraction. Images from time lapse recording of epithelial cells in embryos (stage 7) expressing E-Cad-GFP, injected with **(A)** 2 mM "NP-EGTA, AM" (blue) or **(B)** buffer (purple) and exposed to the UV laser. Scale bar 10 µm. Target cells are highlighted. **(C)** Cross-sectional area of target cells normalized to initial size. Mean (bold line) with standard error of the mean (ribbon band). uncaging, (blue) 8 cells in 8 embryos. Control (purple) 5 cells in 5 embryos. **(D, E)** Cross-sectional area of a target cell (highlighted in blue) with extended recording over 15 minutes after a Ca^{2+} uncaging. Scale bar, 10 µm.

Figure 3: Focal volume of UV exposure affects response time. (A) Target cells were exposed to UV light with a large or small focal volume by adjusting the spot radius. **(B)** Images from time lapse recording of epithelial cells in embryos (stage 7) expressing E-Cad-GFP and injected with 2 mM "NP-EGTA, AM". Two target cells were exposed to the UV laser one after the other with a spot radius of 4 (purple) or 1 (blue). Scale bar 10 µm. **(C)** Traces of cross sectional area of target cells normalized to the

initial area in each three cells in three embryos. Mean (bold) and standard error of mean (ribbon band).

Figure 4: Myosin II dynamics in target cells. Embryos expressing Sqh-mCherry (green) and E-Cadherin-GFP (red) were injected with **(A)** 2 mM "NP-EGTA, AM" injected or **(B)** buffer. Images from time lapse recording in cells of the lateral epidermis in embryos (stage 7) after UV exposure at indicated time. Yellow arrowheads point to target cells. Scale bar 10 µm. **(C)** Quantified medial Sqh-mCherry fluorescence intensity in target cells. The change in fluorescence intensities with reference to fluorescence in the first frame after UV-laser illumination is plotted for the target cells. Mean of three cells in 3 embryos (bold line) and standard error of mean (ribbon).

Figure S1: Area traces of target cells. Traces of cross-sectional cell areas of individual target cells (dashed lines) following UV-laser illumination. **(A)** embryos injected with 2 mM "NP-EGTA, AM" injected embryos (n=8 cells in 8 embryos). **(B)** embryos injected with buffer (n=5 cells in 5 embryos). Mean (bold line) with standard error of mean (ribbon).

Figure S2: Variation of UV exposure. Exposure by large (purple lines, spot radius 4) and small (blue lines, spot radius 1) focal volume of the UV laser. Cross-sectional cell area of target cells after Ca^{2+} uncaging normalized to the initial size. Each line represents one individual cell in one embryo.

References

1. Bertet, C., Sulak, L. & Lecuit, T. Myosin-dependent junction remodelling controls planar cell intercalation and axis elongation. *Nature* **429,** 667–671 (2004).
2. Blankenship, J. T., Backovic, S. T., Sanny, J. S. P., Weitz, O. & Zallen, J. A. Multicellular Rosette Formation Links Planar Cell Polarity to Tissue Morphogenesis. *Developmental Cell* **11,** 459–470 (2006).
3. Heisenberg, C.-P. & Bella che, Y. Forces in Tissue Morphogenesis and Patterning. *Cell* **153,** 948–962 (2013).
4. Martin, A. C. & Goldstein, B. Apical constriction: themes and variations on a cellular mechanism driving morphogenesis. *Development* **141,** 1987–1998 (2014).
5. Hoffman, B. D. & Yap, A. S. Towards a Dynamic Understanding of Cadherin-Based Mechanobiology. *Trends in Cell Biology* **25,** 803–814 (2015).

6. Guglielmi, G., Barry, J. D., Huber, W. & De Renzis, S. An Optogenetic Method to Modulate Cell Contractility during Tissue Morphogenesis. *Developmental Cell* **35,** 646–660 (2015).
7. Valon, L., Marín-Llauradó, A., Wyatt, T., Charras, G. & Trepat, X. Optogenetic control of cellular forces and mechanotransduction. *Nature Communications* **8,** 14396 (2017).
8. Oakes, P. W. *et al.* Optogenetic control of RhoA reveals zyxin-mediated elasticity of stress fibres. *Nature Communications* **8,** 15817 (2017).
9. Lee, H. C. & Auersperg, N. Calcium in epithelial cell contraction. *The Journal of Cell Biology* **85,** 325–336 (1980).
10. Hunter, G. L., Crawford, J. M., Genkins, J. Z. & Kiehart, D. P. Ion channels contribute to the regulation of cell sheet forces during Drosophila dorsal closure. *Development* **141,** 325–334 (2014).
11. Lee, H. & Nagele, R. G. Toxic and teratologic effects of verapamil on early chick embryos: Evidence for the involvement of calcium in neural tube closure. *Teratology* **33,** 203–211 (1986).
12. Smedley, M. J. & Stanisstreet, M. Calcium and neurulation in mammalian embryos. II. Effects of cytoskeletal inhibitors and calcium antagonists on the neural folds of rat embryos. *Journal of Embryology and Experimental Morphology* **93,** 167–178 (1986).
13. Ferreira, M. C. & Hilfer, S. R. Calcium Regulation of Neural Fold Formation: Visualization of the Actin Cytoskeleton in Living Chick Embryos. *Developmental Biology* **159,** 427–440 (1993).
14. He, L., Wang, X., Tang, H. L. & Montell, D. J. Tissue elongation requires oscillating contractions of a basal actomyosin network. *Nature Cell Biology* **12,** 1133–1142 (2010).
15. Suzuki, M. *et al.* Distinct intracellular Ca(2+) dynamics regulate apical constriction and differentially contribute to neural tube closure. *Development* **144,** 1307–1316 (2017).
16. Fehrentz, T., Schönberger, M. & Trauner, D. Optochemical Genetics. *Angewandte Chemie International Edition* **50,** 12156–12182 (2011).
17. Ellis-Davies, G. C. & Kaplan, J. H. Nitrophenyl-EGTA, a photolabile chelator that selectively binds Ca2+ with high affinity and releases it rapidly upon photolysis. *Proceedings of the National Academy of Sciences* **91,** 187–191 (1994).
18. Burgalossi, A. *et al.* Analysis of neurotransmitter release mechanisms by photolysis of caged Ca2+ in an autaptic neuron culture system. *Nature Protocols* **7,** 1351–1365 (2012).
19. Delaney, K. R. & Shahrezaei, V. Uncaging Calcium in Neurons. *Cold Spring Harbor Protocols* **12,** 1115-24 (2013).
20. Chen, T.-W. *et al.* Ultrasensitive fluorescent proteins for imaging neuronal activity. *Nature* **499,** 295–300 (2013).
21. Fernandez-Gonzalez, R. & Zallen, J. A. Oscillatory behaviors and hierarchical assembly of contractile structures in intercalating cells. *Physical Biology* **8,** 045005–14 (2011).
22. Yu, J. C. & Fernandez-Gonzalez, R. Local mechanical forces promote polarized junctional assembly and axis elongation in Drosophila. *eLife* **5,** 20246 (2016).

23. Vicente-Manzanares, M., Ma, X., Adelstein, R. S. & Horwitz, A. R. Non-muscle myosin II takes centre stage in cell adhesion and migration. *Nature Reviews Molecular Cell Biolog* **10,** 778–790 (2009).
24. Martin, A. C., Kaschube, M. & Wieschaus, E. F. Pulsed contractions of an actin|[ndash]|myosin network drive apical constriction. *Nature* **457,** 495–499 (2009).
25. Gramates, L. S. *et al.* FlyBase at 25: looking to the future. *Nucleic Acids Research* **45,** D663–D671 (2017).
26. Huang, J., Zhou, W., Dong, W., Watson, A. M. & Hong, Y. Directed, efficient, and versatile modifications of the Drosophila genome by genomic engineering. *Proceedings of the National Academy of Sciences* **106,** 8284–8289 (2009).
27. Oda, H. & Tsukita, S. Real-time imaging of cell-cell adherens junctions reveals that Drosophila mesoderm invagination begins with two phases of apical constriction of cells. *Journal of Cell Science* **114,** 493–501 (2001).
28. Schindelin, J. *et al.* Fiji: an open-source platform for biological-image analysis. *Nature Methods* **9,** 676–682 (2012).
29. Aigouy, B., Umetsu, D. & Eaton, S. Segmentation and Quantitative Analysis of Epithelial Tissues. *Methods in Molecular Biology* **1478,** 227–239 (2016).
30. Li, K. The image stabilizer plugin for ImageJ. *http://www.cs.cmu.edu/~kangli/code/Image_Stabilizer.html,* (2008).

Figure 1

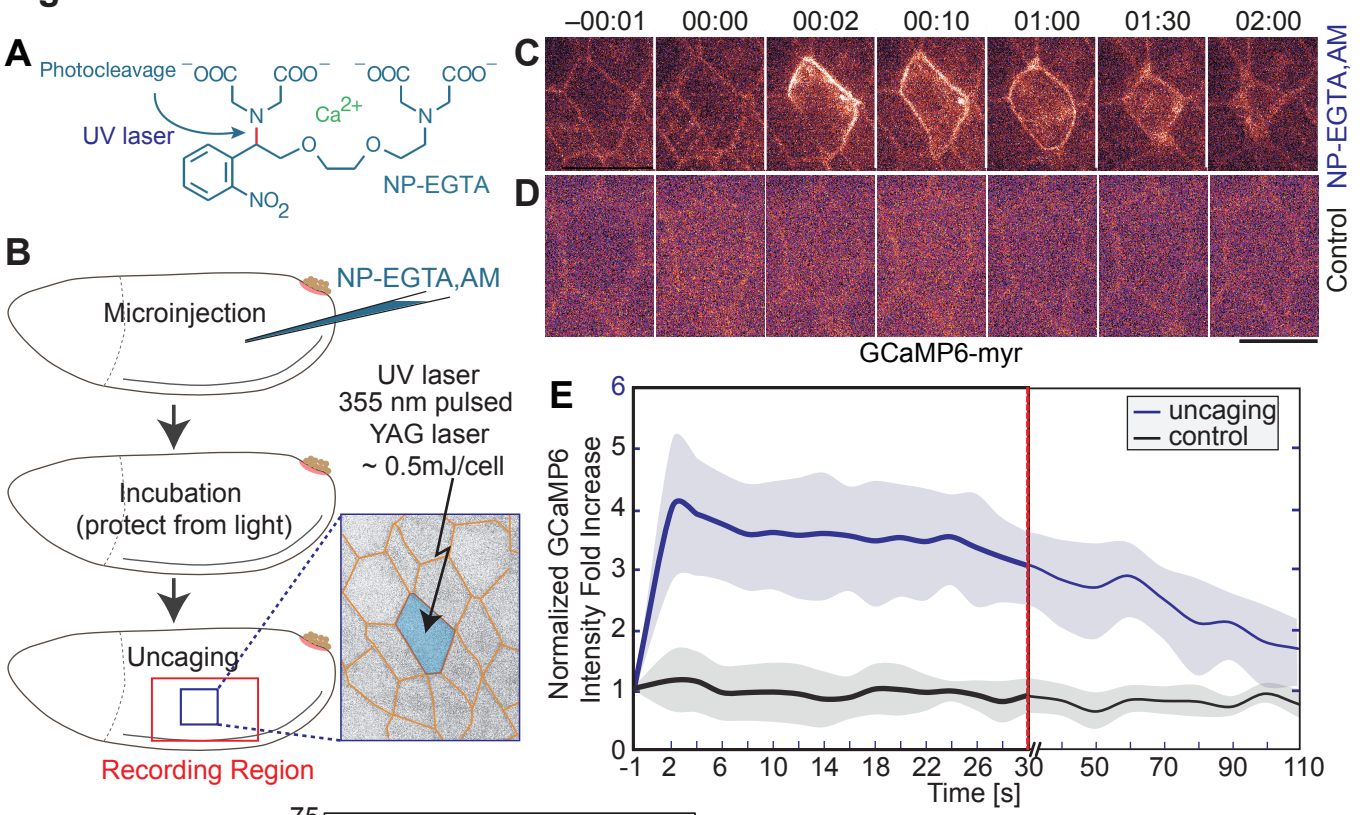

Figure 2

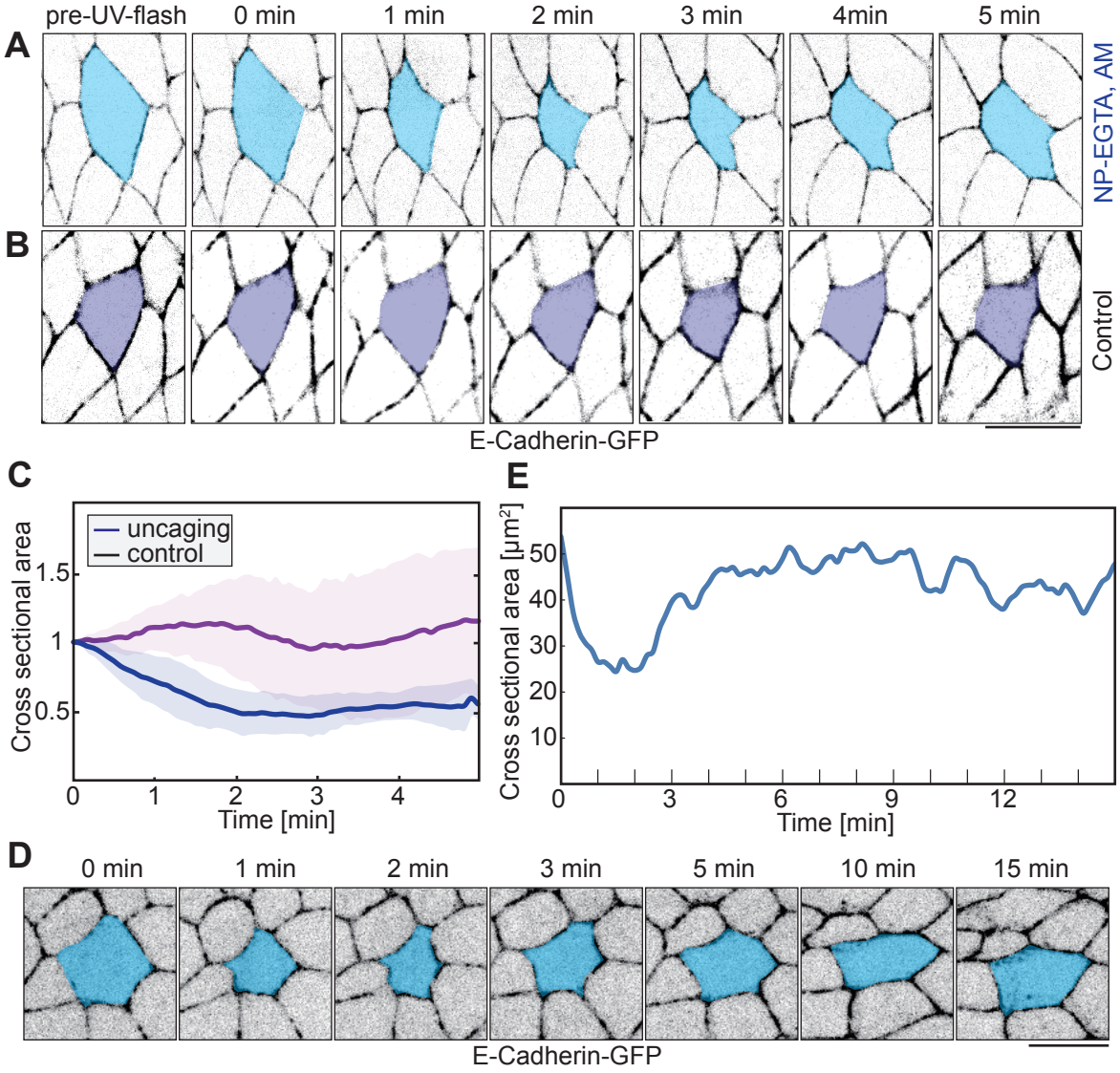

Figure 3

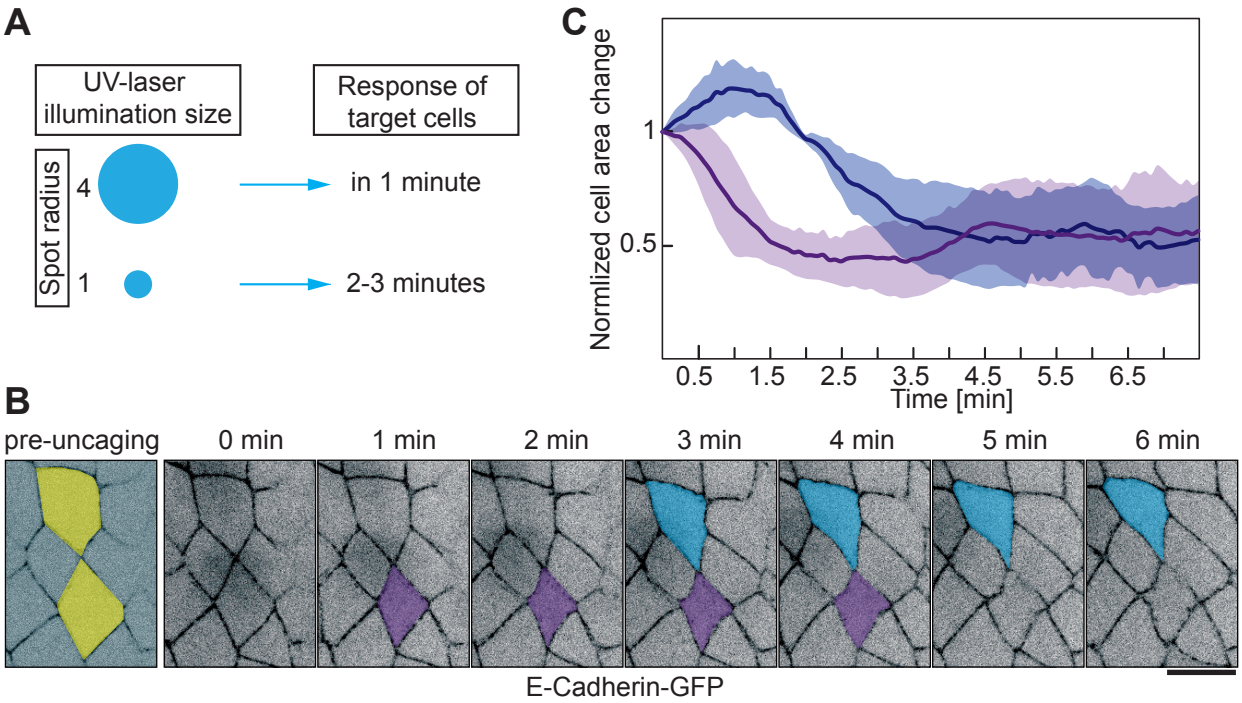

Figure 4

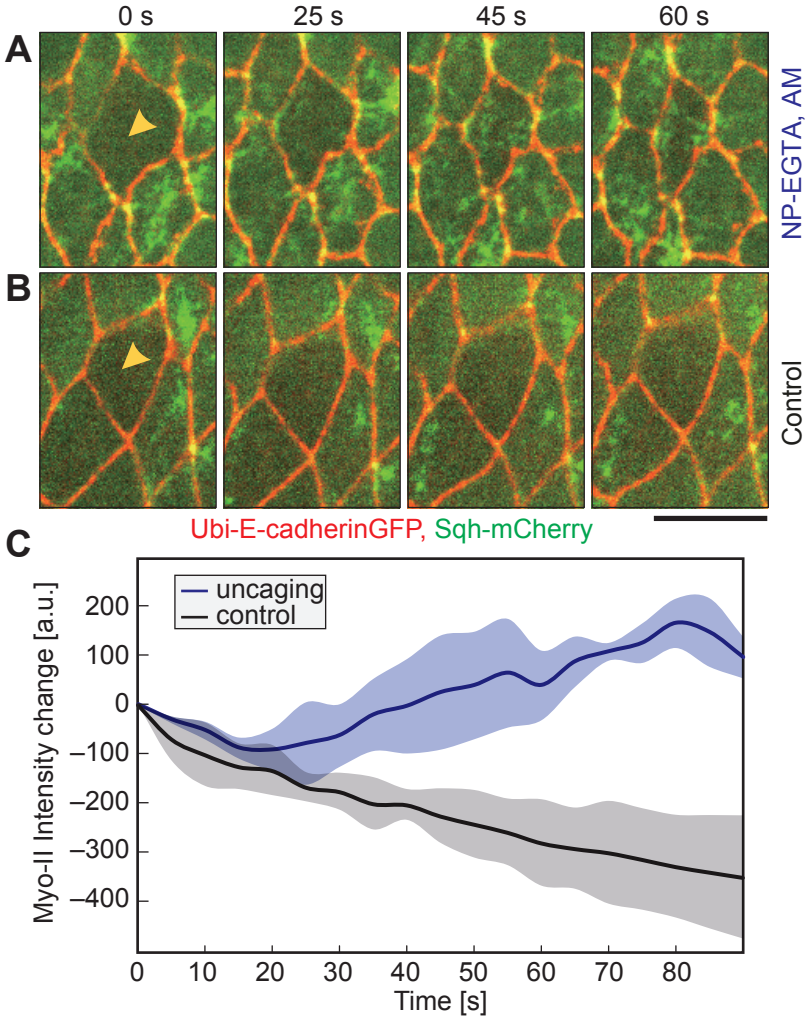

Figure S1

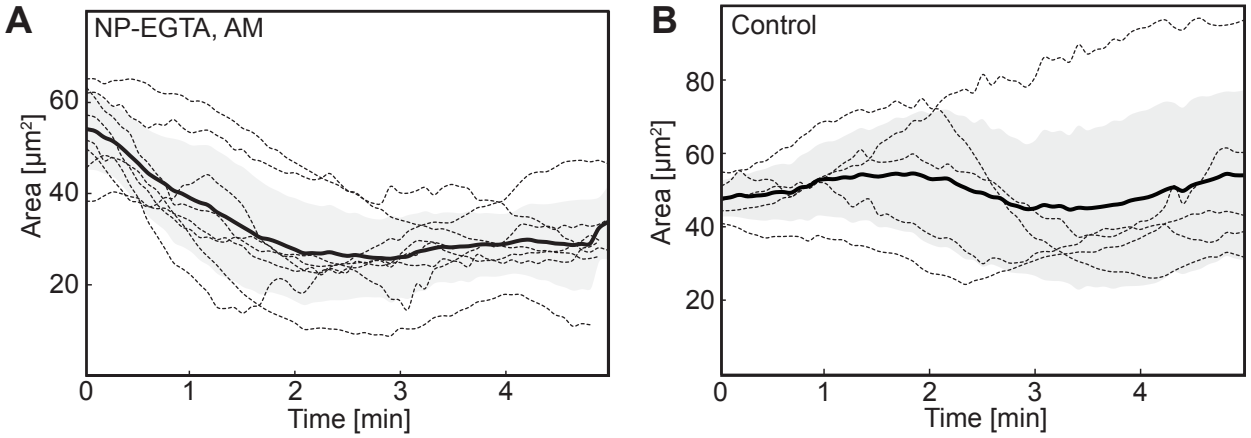

Figure S2